N74-34449

DRAG REDUCTIONS OBTAINED BY MODIFYING A BOX-SHAPED GROUND VEHICLE

Edwin J. Saltzman, et al

NASA Flight Research Center
Edwards, California
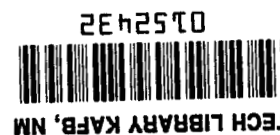
October 1974

KEEP UP TO DATE

Between the time you ordered this report—which is only one of the hundreds of thousands in the NTIS information collection available to you—and the time you are reading this message, several *new* reports relevant to your interests probably have entered the collection.

Subscribe to the **Weekly Government Abstracts** series that will bring you summaries of new reports *as soon as they are received by NTIS* from the originators of the research. The WGA's are an NTIS weekly newsletter service covering the most recent research findings in 25 areas of industrial, technological, and sociological interest—invaluable information for executives and professionals who must keep up to date.

The executive and professional information service provided by NTIS in the **Weekly Government Abstracts** newsletters will give you thorough and comprehensive coverage of government-conducted or sponsored research activities. And you'll get this important information within two weeks of the time it's released by originating agencies.

WGA newsletters are computer produced and electronically photocomposed to slash the time gap between the release of a report and its availability. You can learn about technical innovations immediately—and use them in the most meaningful and productive ways possible for your organization. Please request NTIS-PR-205/PCW for more information.

The weekly newsletter series will keep you current. But *learn what you have missed in the past* by ordering a computer **NTISearch** of all the research reports in your area of interest, dating as far back as 1964, if you wish. Please request NTIS-PR-186/PCN for more information.

WRITE: Managing Editor
5285 Port Royal Road
Springfield, VA 22161

Keep Up To Date With SRIM

SRIM (Selected Research in Microfiche) provides you with regular, automatic distribution of the complete texts of NTIS research reports *only* in the subject areas you select. SRIM covers almost all Government research reports by subject area and/or the originating Federal or local government agency. You may subscribe by any category or subcategory of our WGA **(Weekly Government Abstracts)** or **Government Reports Announcements and Index** categories, or to the reports issued by a particular agency such as the Department of Defense, Federal Energy Administration, or Environmental Protection Agency. Other options that will give you greater selectivity are available on request.

The cost of SRIM service is only 45¢ domestic (60¢ foreig) for each complete microfiched report. Your SRIM service begins as soon as your order is received and processed and you will receive biweekly shipments thereafter. If you wish, your service will be backdated to furnish you microfiche of reports issued earlier.

Because of contractual arrangements with several Special Technology Groups, not all NTIS reports are distributed in the SRIM program. You will receive a notice in your microfiche shipments identifying the exceptionally priced reports not available through SRIM.

A deposit account with NTIS is required before this service can be initiated. If you have specific questions concerning this service, please call (703) 451-1558, or write NTIS, attention SRIM Product Manager.

This information product distributed by

NTIS U.S. DEPARTMENT OF COMMERCE
National Technical Information Service
5285 Port Royal Road
Springfield, Virginia 22161

NASA TM X-56027

DRAG REDUCTIONS OBTAINED BY MODIFYING A BOX-SHAPED

GROUND VEHICLE

Edwin J. Saltzman, Robert R. Meyer, Jr., and David P. Lux

October 1974

(NASA-TM-X-56027) DRAG REDUCTIONS
OBTAINED BY MODIFYING A BOX-SHAPED GROUND
VEHICLE (NASA) 29 p HC $3.25 CSCL 01A

N74-34449

G3/01 Unclas 51021

NASA Flight Research Center
Edwards, California 93523

1 Report No. TM X-56027	2 Government Accession No.	3 Recipient's Catalog No.
4 Title and Subtitle DRAG REDUCTIONS OBTAINED BY MODIFYING A BOX-SHAPED GROUND VEHICLE		5 Report Date October 1974
		6 Performing Organization Code
7 Author(s) Edwin J. Saltzman, Robert R. Meyer, Jr., and David P. Lux		8 Performing Organization Report No
9 Performing Organization Name and Address NASA Flight Research Center P. O. Box 273 Edwards, California 93523		10 Work Unit No 770-18-10
		11 Contract or Grant No
12 Sponsoring Agency Name and Address National Aeronautics and Space Administration Washington, D C. 20546		13 Type of Report and Period Covered Technical Memorandum
		14 Sponsoring Agency Code

15 Supplementary Notes

16 Abstract

A box-shaped ground vehicle was used to simulate the aerodynamic drag of high volume transports, that is, delivery vans, trucks, or motor homes. The coast-down technique was used to define the drag of the original vehicle, having all square corners, and several modifications of the vehicle. Test velocities ranged up to 65 miles per hour, which provided maximum Reynolds numbers of 1×10^7 based on vehicle length. One combination of modifications produced a reduction in aerodynamic drag of 61 percent as compared with the original square-cornered vehicle.

PRICES SUBJECT TO CH...

17 Key Words (Suggested by Author(s)) Aerodynamic drag: Ground vehicle Truck Automotive Bluff shape Aerodynamic drag reduction		18 Distribution Statement Unclassified - Unlimited		
19 Security Classif (of this report) Unclassified	20 Security Classif. (of this page) Unclassified		21 No of Pages 27	22 Price*

*For sale by the National Technical Information Service
Springfield, Virginia 22151

DRAG REDUCTIONS OBTAINED BY MODIFYING A

BOX-SHAPED GROUND VEHICLE

Edwin J. Saltzman, Robert R. Meyer, Jr., and
David P. Lux
Flight Research Center

INTRODUCTION

Recent increases in the price of gasoline and diesel fuel, and uncertainty regarding future fuel supplies, have resulted in widespread interest in increasing the efficiency of ground vehicles. There are several approaches worthy of study in this regard. Prominent among these is the possibility of reducing aerodynamic drag.

There are substantial amounts of data concerning the drag of subscale models of automobiles, techniques for testing such models, and ways to estimate full-scale vehicle drag (refs. 1 to 10). Some studies have also been made with truck-like shapes (refs. 11 to 14).

Results from a box-shaped vehicle (ref. 15) indicate that substantial differences sometimes exist between the drag characteristics of highway-sized rolling vehicles and similarly shaped subscale models. In light of these findings, and because high volume box-like shapes are aerodynamically inefficient, further work has been done with modified versions of the vehicle described in reference 15. The modifications consisted of rounding the horizontal and vertical corners of the front of the vehicle, rounding these corners on the rear of the vehicle, sealing the bottom of the chassis with a full-length fairing and then using a 3/4-length underbody fairing. Drag results from these configurations are compared with the reference 15 data for the vehicle with all corners square and vertical corners rounded.

Test velocities ranged up to 65 miles per hour and the corresponding Reynolds numbers ranged up to 1×10^7 based on vehicle length. A simple coast-down technique was used to define the drag.

SYMBOLS

A body cross-sectional reference area (same for all configurations)

C_{d_a} aerodynamic drag coefficient, $\dfrac{D_a}{qA}$

C_{P_b} base pressure coefficient, $\dfrac{\Delta P_b}{q}$

D_a aerodynamic drag

ΔD increment of aerodynamic drag

$D_{a_\square}$ aerodynamic drag for configuration A having all corners square

D_m mechanical drag

D_t total drag

g local acceleration of gravity

ℓ vehicle length

P ambient pressure

P_b base pressure

$\Delta P_b = P_b - P$

q dynamic pressure, $0.5\rho V_c^2$

R Reynolds number based on vehicle length, $\dfrac{\rho V_c \ell}{\mu}$

r radius of rounded corners, vertical or horizontal

Δt time increment

V_c calibrated velocity

ΔV_c velocity increment

W vehicle weight for each test

w width of vehicle

μ absolute viscosity

ρ air density

VEHICLE CONFIGURATIONS

The test vehicle used for this series of configurations is the same basic vehicle as described in reference 15. The various configurations were achieved by relatively simple changes to sheet metal that was affixed to the subframe of the carrier vehicle as described in reference 15. The various configurations are as follows:

Configuration	Corners		Underbody
	Front	Rear	
A	Square	Square	Exposed
B	Vertical rounded, horizontal square	Vertical rounded, horizontal square	Exposed
C	Rounded	Rounded	Exposed
D	Rounded	Rounded	Full-length seal
E	Rounded	Rounded	3/4-length seal
I	Rounded	Square	3/4-length seal

Configurations A and B were the subject of study in reference 15. All the configurations had the same length and the same frontal area. These dimensions can be obtained from figure 1.

Configurations With Underbody Exposed

Configuration A, with all corners square, is shown in figure 2, and configuration B, with rounded vertical corners in the front and rear, is shown in figure 3. The radius of the rounded corners for configuration B was equal to 20 percent of the vehicle width, that is, $\dfrac{r}{w} = 0.2$. Configuration C, in which all (horizontal and vertical, front and rear) corners were rounded, is shown in figure 4. All rounded corners for configuration C had an $\dfrac{r}{w}$ ratio of 0.2.

The underbody of configurations A, B, and C was exposed; that is, the front suspension system, transmission, driveline, rear axle, differential, and other underbody parts were exposed to the air that flowed underneath the vehicle. A photograph of the exposed underbody that was taken before the sheet metal shell was attached to the vehicle is shown in figure 5.

Configurations With Underbody Sealed

Configurations D, E, and F had a partially or fully sealed underbody. Except for the underbody, configurations D and E were the same as configuration C. The full-length underbody seal of configuration D and the 3/4-length seal of configuration E are shown in figures 6(a) and 6(b) as seen from a viewer position similar to the exposed underbody photograph of figure 5. Further details pertaining to the underbody seal will be given in a following subsection.

Configuration F (fig. 7) had the same rounded corners in front as configurations C, D, and E and a blunt aft end with all corners square like configuration A. F had the 3/4-length underbody seal used on configuration E.

Underbody Seal

The full-length underbody seal was configured so that it faired smoothly into the front and rear lower horizontal rounded corners. An aft-facing gap underneath the vehicle permitted the cooling air that passed through the engine radiator to escape during cooling vent open operation. This gap is shown from behind the gap and from the left of the left wheels in figure 8(a). A somewhat similar view of the exposed underbody is shown in figure 8(b).

The wheel wells were sealed for configurations D, E, and F. They were unsealed for configurations A, B, and C. Figure 9(a) shows the front wheel well seal which was made of fiber glass cloth and tape to allow the front suspension system to flex. Figure 9(b) shows the same front wheel well before the underbody and wheel well seals were installed.

Sheet metal and tape were used to seal the rear wheel wells. Figure 10(a) shows the right rear wheel well seal installation viewed from somewhat behind the axle. Figure 10(b) shows the left rear wheel well before the installation of the wheel well seal, also viewed from behind the axle. A portion of the bottom seal and a former between the bottom seal and the axle are visible below the axle. Although the rear wheel well seals were in place for configurations D, E, and F, the full-length bottom seal was installed only for configuration D.

Configuration D was unique in another way. As the former and sheet metal fairing visible in figure 10(b) suggest, the full-length seal impaired the freedom of movement of the rear suspension system. To prevent the rear part of the underbody seal from buckling, the rear suspension motion was eliminated by tying the axle to the chassis with two heavy shackles. The shackles were removed for configurations E and F because the underbody seal terminated immediately in front

of the rear wheels. Vertical slots were provided in the rear wheel seals for configurations E and F to allow the rear axle to respond to road discontinuities without damaging the seals.

TEST PROCEDURE

Method and Test Conditions

The coast-down method was used to obtain the total drag of the vehicle. Total drag is used here to mean the sum of the aerodynamic drag, the tractive drag of the tires and bearings, the gear resistance back through the drive line to the transmission, and the thrust from the rotational inertia of the wheels, tires, and other parts of the drive line. The coast-down method is described in references 16 to 18, and the specific approach taken for the present investigation is described in reference 15.

Most of the test runs were made on the runway used to investigate configurations A and B (ref. 15). This runway is exceptionally smooth and has an elevation gradient of only 0.08 percent; the effects of gradient were eliminated by averaging runs made in opposite directions. This procedure also compensated for the effects of winds. Testing was cancelled when winds exceeded 2 to 3 knots along the runway, or 5 to 6 knots across the runway; however, most of the tests were made early in the day when it was calm. The most common wind condition that was encountered, when there were winds, was a cross wind of up to 2 or 3 knots.

Wind velocity and direction, ambient pressure, and temperature were monitored and documented for each day of testing so that the effects of these factors could be taken into account. The vehicle was weighed, with occupants, after each day's testing to provide the proper mass for computing drag. The vehicle began each day of testing with a tire pressure of 38 pounds per square inch. All the results presented in this report and in reference 15 represent the cooling vent closed condition. The cooling vent is shown open and closed in figures 2 and 3, respectively.

Instrumentation

Deceleration.— Two methods were used to define the vehicle's deceleration for the investigation described in reference 15 — the speedometer-stopwatch method and a backup accelerometer-oscillograph method. The accelerometer readings were influenced by the depression of the front suspension system during deceleration, so with the accelerometer-oscillograph method corrections were necessary to define the actual rate of change of forward velocity. The speedometer-stopwatch method provided the absolute value of the rate of change of velocity more directly and was more convenient, so it was the only method used for this investigation.

Base pressure.— Base pressure measurements, which were required for configurations E and F only, were made by using a precision direct reading absolute aneroid dial barometer. Tare readings were made at zero velocity on the portion of the runway where data runs were made so that runway elevation gradient effects were eliminated. Then data runs were made repeatedly in both directions past the tare location. Tare readings were interspersed between the data runs to provide a history of tare pressure for zero velocity as a function of time. By knowing the time of each data run, the appropriate absolute tare value was applied and the ΔP_b for a given velocity was obtained.

A backup measurement of base pressure was made by using a differential pressure transducer sensor that was referenced to a flush orifice located near the middle of the top surface of the vehicle. The transducer output was recorded on an oscillograph. The backup method confirmed the results from the aneroid barometer.

RESULTS

Tuft Patterns

Tuft patterns for configurations A, B, and C for a calibrated speed of 55 miles per hour are shown in figures 11(a), 11(b), and 11(c), respectively, for the cooling vent closed. Figure 11(a) shows that for the square-cornered configuration the flow separates just behind the front vertical corner and that completely attached flow is not achieved anywhere along the side. A corresponding photograph showing the top surface of configuration A is not available; however, a photograph of the tuft pattern at the top forward edge of configuration A (fig. 12) suggests a condition of separated flow similar to the side's. Figures 11(b) and 11(c) show that flow is attached with rounded corners over all the surfaces in view. The flow remained attached over the forwardmost portion of the rear rounded corners. The tuft patterns for each configuration were the same whether the cooling vent was open or closed except for the region immediately adjacent to the opening.

Total Drag

Total drag results for configurations A to D are presented in figure 13. The total drag was derived from measurements of coasting deceleration, which includes the effects of mechanical factors as well as aerodynamic resistance, as follows:

$$D_t = D_m + D_a = \frac{\Delta V_c}{\Delta t} \cdot \frac{W}{g}$$

where the mechanical drag, D_m, consists of the tractive drag of the rotating parts from the tires, back through the driveline to the transmission, and the thrust from the rotation inertia of these parts. The symbol at $V_c \approx 1$ in figure 13 is the low-limit tractive drag measured for the vehicle for tire pressures between 38 pounds

per square inch and 40 pounds per square inch. The heavy dashed curve is an extrapolation for velocity effects on tractive drag that is based on a semiempirical equation from reference 1. The extrapolation provided by this expression was derived by Hoerner (ref. 1) for tire characteristics of the 1930's and 1940's; however, it has been found to provide velocity effects that agree with modern tires of the type used in this experiment (refs. 18 to 20).

Figure 13 and the following table show the improvement in performance (that is, speed capability) due to the increasing aerodynamic refinement of configurations B, C, and D as compared with A. Indexes of 200 pounds of total drag and 34 horsepower were chosen arbitrarily to demonstrate the velocity obtainable by each configuration, within these indexes.

Configuration	V_c for D_t = 200 lb, mph	V_c for 34 horsepower, mph
A	39.5	47.5
B	48.5	54.5
C	56.0	59.5
D	63.5	63.5

Thus, rounding the horizontal and vertical corners (configuration C) increased the velocity for 200 pounds of total drag by approximately 42 percent and the velocity for 34 horsepower by 25 percent compared with the configuration with all corners square (configuration A). The addition of the underbody seal (configuration D) provided corresponding velocity increases of approximately 60 percent and 34 percent, respectively.

Aerodynamic Drag

The aerodynamic drag of each configuration was calculated by subtracting the extrapolated tractive drag from the total drag and accounting for the calculated effects of rotational inertia. The resulting aerodynamic drag coefficients for each configuration with the cooling vent closed are summarized in the following table, which is for a calibrated speed of 60 miles per hour; the nonparabolic curves (configurations C and D) in figure 13 indicated that these values of drag coefficient apply only at this speed.

Configuration	C_{D_a}	$\frac{\Delta D_a}{D_{a_\square}}$, percent
A	1.13	0
B	0.68	40
C	0.520	54
D	0.440	61
E	0.443	61
F	0.463	59

The configuration with all corners square (configuration A) had an aerodynamic drag coefficient of 1.13, significantly higher than the model values of 0.86 (ref. 1) and 0.93 (ref. 12). As mentioned in reference 15, this difference is believed to be caused primarily by the exposed underbody protuberances of the actual test vehicle, which were not adequately simulated by the models.

Configuration B provided a 40-percent reduction in aerodynamic drag as compared with configuration A, and the corresponding reductions provided by configurations C and D were 54 percent and 61 percent, respectively.

Configurations C, D, E, and F had aerodynamic drag coefficients close to those of conventional automobiles, as is apparent from a comparison of the values of C_{D_a} in the table with those in figure 14. The figure, which is adapted from reference 9, shows the trend of C_{D_a} with automobile type. References 4, 5, and 10 confirm this finding. Thus, although a modern automobile has an appearance of sleekness, its aerodynamic drag coefficient is in most cases about the same as a relatively clean box with its forward corners rounded.

A comparison of configurations C and D shows that the full-length underbody seal reduced aerodynamic drag approximately 15 percent. Similar results were obtained with a 3/8-scale model of a conventional automobile with the flow through the radiator blocked (ref. 5). The reduction in aerodynamic drag provided by the 3/4-length seal (configuration E) was also approximately 15 percent. This result is in general agreement with the model data from reference 5, which showed that the difference in drag between an automobile model with a full-length seal and one with a seal with the aft third removed was negligible.

Underbody seals like those of configurations D or E may result in even greater reductions in drag for full-scale family sedans or station wagons than they did for the configurations tested, assuming that the automobile's exposed underbody is similar to that shown in figure 5. This possibility exists because the frontal area of an ordinary automobile is small compared with that of the configurations tested, which means that a similar reduction in drag would be larger in proportion to the vehicle's overall aerodynamic drag.

The design of the underbody seal used in this investigation, although effective in terms of reducing drag, would require changes in detail to be practical for general use. For example, the heat from the exhaust system was trapped between the seal and the floor of the carrier vehicle. In addition, the seal was difficult to remove, which complicated routine maintenance from underneath. Each of these problems should yield to a thoughtful design effort, however.

Rounding the corners obviously results in a loss of usable volume. For configuration B, the loss in volume was 1.4 percent as compared with configuration A. The corresponding volume loss for configurations C, D, and E was 3.0 percent, and for configuration F it was 1.5 percent.

This study was limited to the coast-down method of sensing drag, which in and of itself does not define the fuel consumption, or fuel mileage, of the respective configurations. Therefore, the demonstrated reductions in drag will not be evaluated quantitatively in terms of savings in fuel. However, references 2, 14, and 21 to 23, among others, suggest that at highway speeds fuel savings in percent are between one-third and one-half of the magnitude of the percentage of reduction in aerodynamic drag. This depends on such factors as the vehicle's configuration, loading, the route, the type of driving, and the presence of wind.

The only difference between configurations E and F is that the back four corners of configuration F were square; therefore, the base of the vehicle was completely flat. This permitted a cursory examination to be made of the cost in drag of the flat base, which is common on trucks. It is understood that these flat bases are advantageous in terms of ease of fabrication and rear door size and secondarily in terms of volume.

The drag penalty of configuration F as compared with configuration E as determined from the deceleration data was approximately 5 percent at 60 miles per hour for calm wind conditions. This corresponds to an increase in aerodynamic drag coefficient of 0.02. These data suggest that a vehicle with only the four front corners rounded and an exposed underbody (in other words, configuration C with a flat base) would have an aerodynamic drag coefficient of approximately 0.54 at 60 miles per hour, which would represent a saving of about one-half in aerodynamic drag compared with configuration A. Thus, the penalty of a flat base is relatively small for calm wind conditions. Limited experience with configurations E and F suggest, however, that the vehicle with the flat base was more sensitive to crosswinds than it was with a rounded base, and with the resultant velocity component displaced 5° or 6°, the aerodynamic drag coefficient of configuration F increased from approximately 0.46 to 0.49. Thus, as is often done, it is good design practice to round the rear corners of buses and motor homes, which do not require a large door at the base.

The drag penalty associated with having square aft corners was also evaluated by making base pressure measurements on configurations E and F. The base pressure coefficients, C_{p_b}, were −0.24 for the rounded base (configuration E) and −0.30 for the square-cornered base (configuration F). The pressure coefficient for the base with rounded corners represents only the flat portion of the base.

Base pressure data from three variations of a wind-tunnel model that simulated box-shaped ground vehicles and did not have wheels or wheel wells are compared in the following table with the base pressures obtained for configurations E and F:

Vehicle	Configuration	R	$\left(\dfrac{r}{w}\right)_{base}$	C_{p_b}
Actual	E F	1×10^7	0.2 0	−0.24 −0.30
Model	- -	2.3×10^6	0.3 0.1 0	−0.20 −0.20 −0.30

The base pressure coefficients from the vehicle of the present study and those from the reference 24 wind-tunnel model tend to agree.

CONCLUDING REMARKS

A box-shaped ground vehicle was used to simulate the aerodynamic drag of high volume transports like delivery vans, trucks, or motor homes. Measurements were made on the vehicle in its original configuration, in which all corners were square, and several modifications of this configuration. The coast-down technique was used at test velocities ranging up to 65 miles per hour. The maximum Reynolds number was 1×10^7 based on vehicle length.

Rounding both the front and the rear corners resulted in a 54-percent reduction in aerodynamic drag at 60 miles per hour as compared to the configuration with all corners square. With the addition of a full-length underbody seal, the drag reduction increased to 61 percent.

The full-length underbody seal provided an incremental reduction in aerodynamic drag of approximately 15 percent for the configuration to which it was applied. The 3/4-length underbody seal also provided a reduction in drag of approximately 15 percent.

The penalty in aerodynamic drag of having square instead of rounded corners at the rear of the vehicle was approximately 5 percent at 60 miles per hour for zero wind conditions.

The configuration with all corners square had a significantly higher drag coefficient than generally similar small-scale models. The higher drag coefficients for the actual vehicle are believed to be caused primarily by underbody protuberances, which were not simulated by the models.

Flight Research Center
National Aeronautics and Space Administration
October 1, 1974

REFERENCES

1. Hoerner, Sighard F.: Fluid-Dynamic Drag. Publ. by the author (148 Busteed Dr., Midland Park, N. J.), 1965.

2. Schlichting, H.: Aerodynamic Problems of Motor Cars. AGARD Rept. 307, Oct. 1960.

3. Larrabee, E. Eugene: Small Scale Research in Automobile Aerodynamics. SAE 660384, 1966.

4. Gross, Donald S.; and Sekscienski, William S.: Some Problems Concerning Wind Tunnel Testing of Automotive Vehicles. SAE 660385, 1966.

5. Turner, Thomas R.: Wind-Tunnel Investigation of a 3/8-Scale Automobile Model Over a Moving-Belt Ground Plane. NASA TN D-4229, 1967.

6. Brown, Glen J.; and Seemann, Gerald R.: The Highway Aerodynamic Test Facility. AIAA Paper No. 72-1000, Sept. 13-15, 1972.

7. Metz, L. Daniel; and Sensenbrenner, Kenneth: The Influence of Roughness Elements on Laminar to Turbulent Boundary Layer Transition as Applied to Scale Model Testing of Automobiles. SAE 730233, 1973.

8. Mason, William T., Jr.; Beebe, Paul S.; and Schenkel, Franz K.: An Aerodynamic Test Facility for Scale-Model Automobiles. SAE 730238, 1973.

9. Cornish, J. J. III; and Fortson, C. B.: Aerodynamic Drag Characteristics of Forty-Eight Automobiles. Res. Note No. 23, Dept. Aerophysics, Mississippi State Univ., June 1964.

10. White, R. G. S.: A Method of Estimating Automobile Drag Coefficients. SAE 690189, 1969.

11. Sherwood, A. Wiley: Wind Tunnel Test of Trailmobile Trailers. Wind Tunnel Rept. No. 85, Univ. Maryland, June 1953.

12. Flynn, Harold; and Kyropoulos, Peter: Truck Aerodynamics. SAE Transactions 1962, Vol. 70, c.1962, pp. 297-308.

13. Kirsch, Jeffrey W.; Garg, Sabodh K.; and Bettes, William: Drag Reduction of Bluff Vehicles With Airvanes. SAE 730686, 1973.

14. Ritchie, Dave: How To Beat the Built-In Headwind. Owner Operator, May-June 1973, pp. 89-99.

15. Saltzman, Edwin J.; and Meyer, Robert R., Jr.: Drag Reduction Obtained by Rounding Vertical Corners on a Box-Shaped Ground Vehicle. NASA TM X-56023, 1974.

16. White, R. A.; and Korst, H. H.: The Determination of Vehicle Drag Contributions from Coast-Down Tests. SAE 720099, 1972.

17. Roussillon, G.; Marzin, J.; and Bourhis, J.: Contribution to the Accurate Measurement of Aerodynamic Drag by the Deceleration Method. Paper 4 of Advances in Road Vehicle Aerodynamics, H. S. Stephens, ed. (BHRA Fluid Engineering, Cranfield, Bedford MK 43 OAJ, Eng.), 1973, pp. 53-62.

18. Dayman, Bain, Jr.. Effects of Realistic Tire Rolling Resistance Upon the Determination of Aerodynamic Drag From Road-Vehicle Coast-Down Tests. Paper presented at Second AIAA Symposium on the Aerodynamics of Sports and Competition Automobiles, Los Angeles, Calif., May 11, 1974.

19. Curtiss, W. W.: Low Power Loss Tires. SAE 690108, 1969.

20. Walters, Joseph D.; and Conant, F. S.: Energy Losses in Tires. Paper presented at Am. Soc. for Testing Materials Committee F-9 Symposium (Dearborn, Mich.), May 8, 1974. (Available from The Firestone Tire & Rubber Co., Central Research Laboratories, Akron, Ohio 44317.)

21. Burke, Carl E.; Nagler, Larry H.; Campbell, E. C.; Zierer, W. E.; Welch, H. L.; Lundstrom, L. C.; Kosier, T. D.; and McConnell, W. A.: Where Does All the Power Go? SAE Transactions, Vol. 65, 1957, pp. 713-738.

22. Austin, Thomas C.; and Hellman, Karl H.: Passenger Car Fuel Economy-Trends and Influencing Factors. SAE 730790, 1973.

23. LaPointe, Clayton: Factors Affecting Vehicle Fuel Economy. SAE 730791, 1973.

24. Carr, G. W.: The Aerodynamics of Basic Shapes for Road Vehicles. Rept. No. 1968/2, Part 1, Simple Rectangular Bodies. The Motor Industry Research Assn., Nov. 1967.
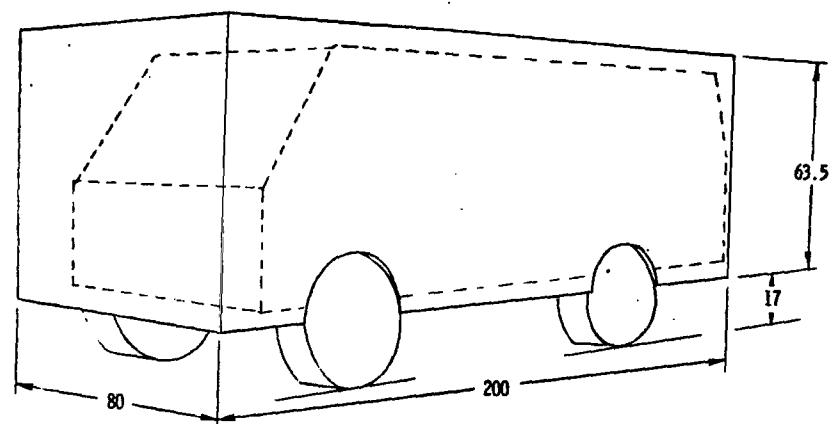
Figure 1. Dimensions (in inches) of square-cornered configuration of test vehicle.
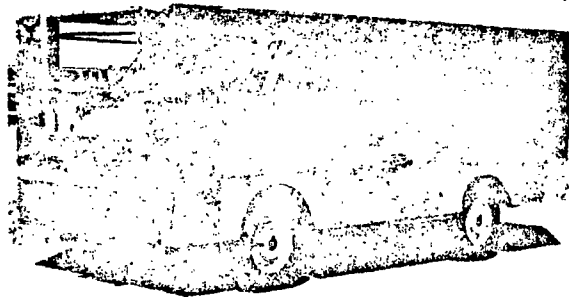
E-26577
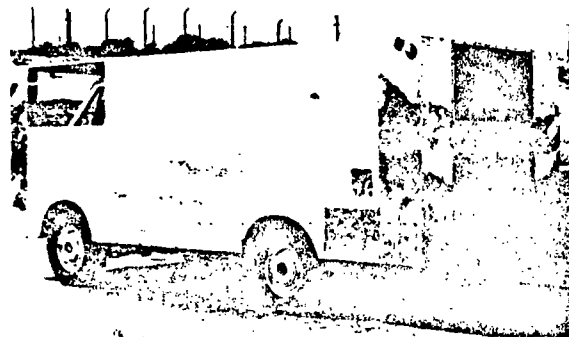
E-26776

E-26575

E-26774

Figure 2. Configuration A. All corners square. Cooling vent open.
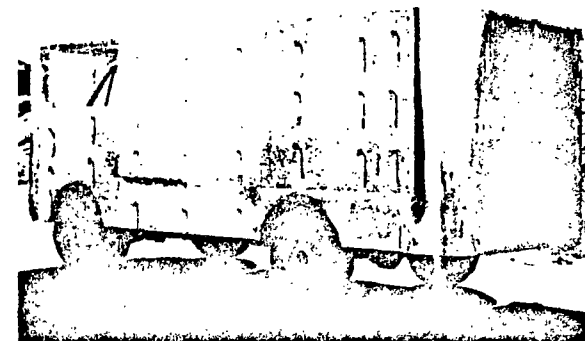
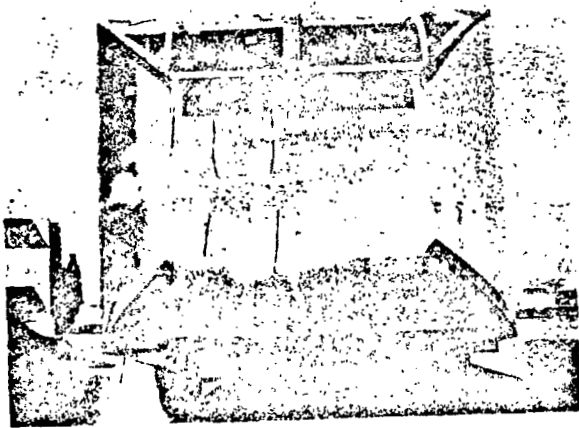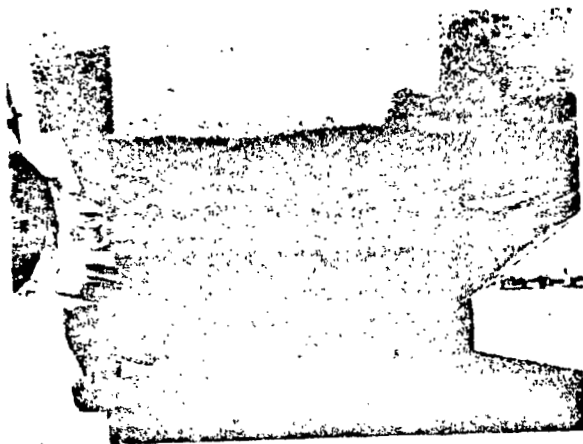Figure 3. Configuration B. Rounded front and rear vertical corners. Cooling vent closed.
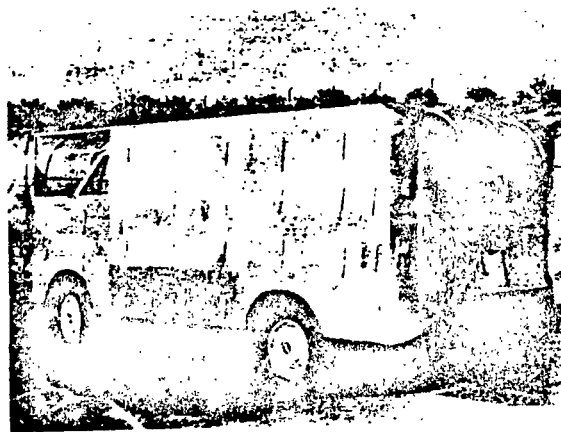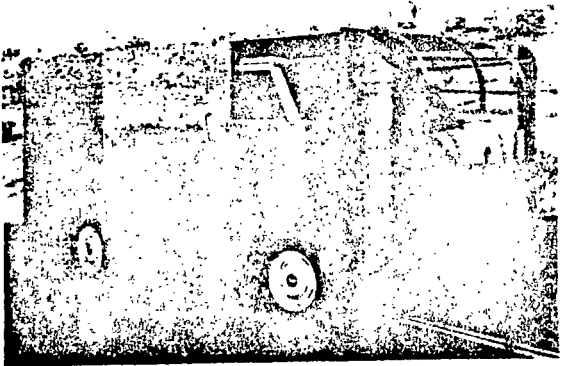
Figure 4. Configuration C. Rounded front and rear horizontal and vertical corners. Cooling vent closed.
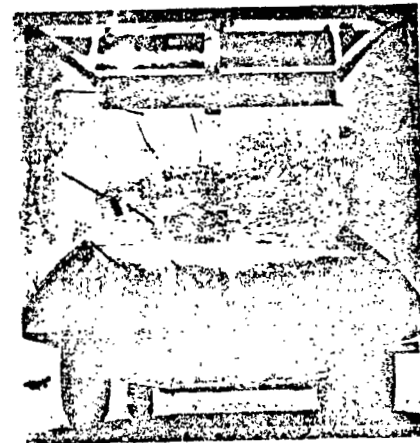
Figure 5. Exposed underbody looking rearward.

E-27716
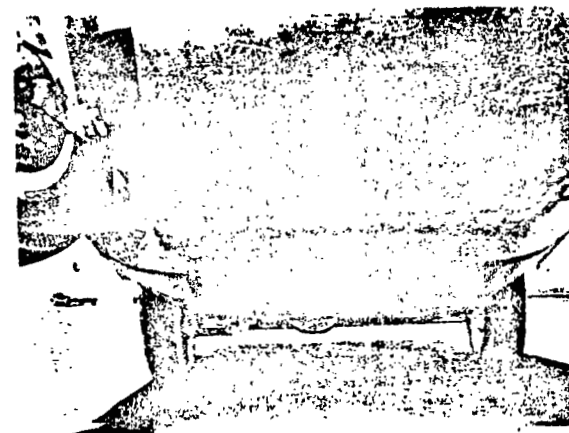
E-27367

E-27365

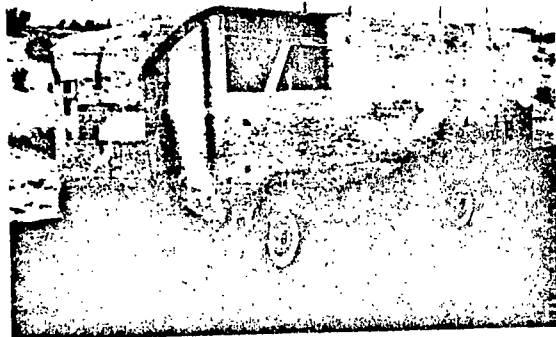(c. Full-length seal. Configuration D.

Figure 6. Sealed underbody looking rearward.

E-27625

E-27626

(b) 3/4-length seal. Configuration E.

Figure 6. Concluded.

E-27719
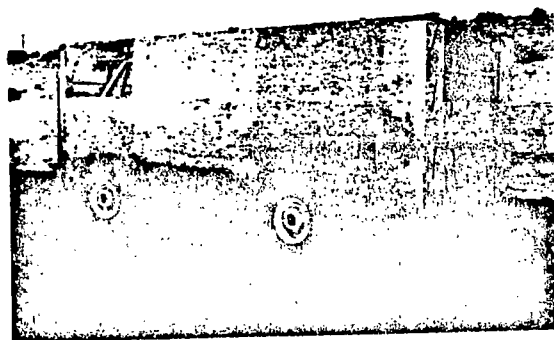
E-27718

Figure 7. Configuration F. Rounded horizontal and vertical corners in front, square corners at the rear. Cooling vent closed.

(a) Air gap for sealed underbody. Configurations D, E, and F.

Figure 8. View beneath front wheels looking forward.
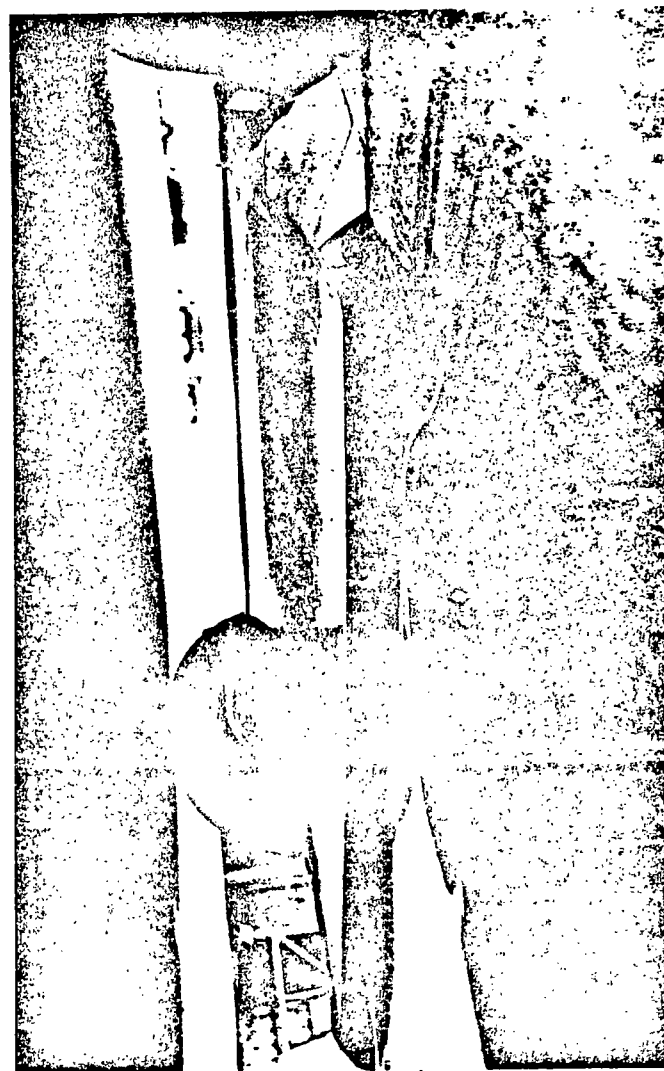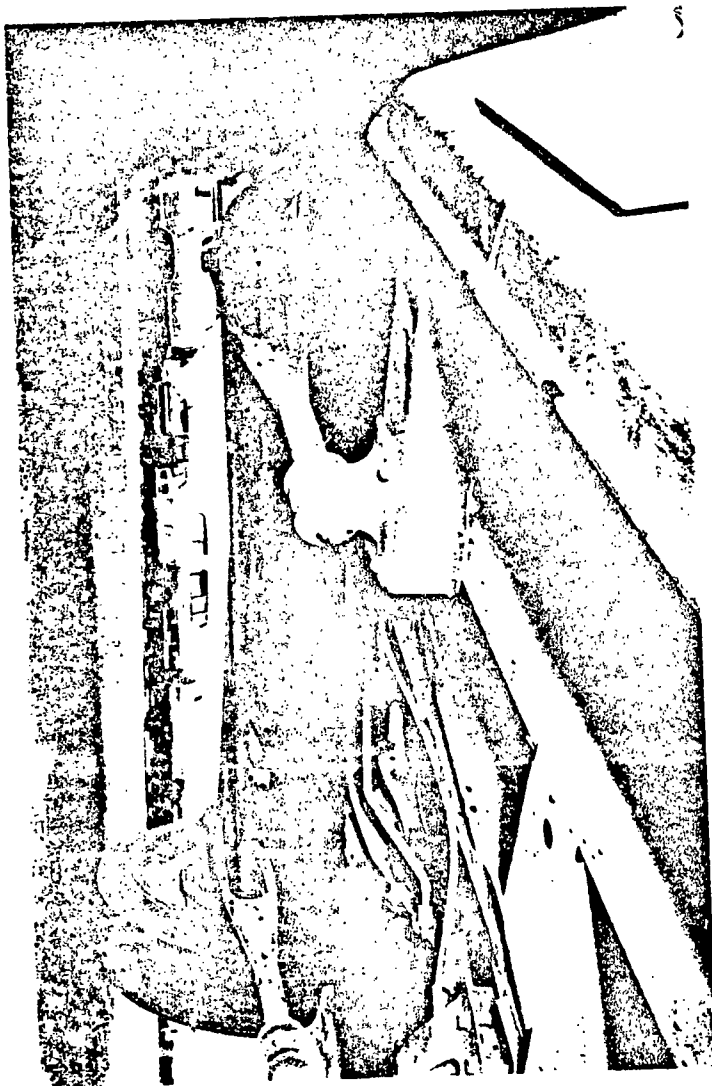
E-27364

(b) Exposed underbody. Configurations A, B, and C.

E-27720

Figure 8. Concluded.
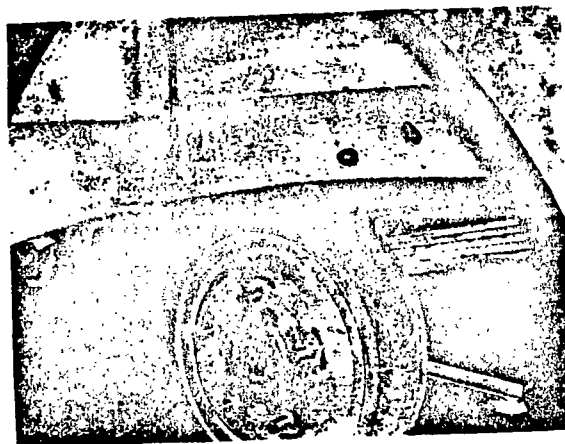
(a) Sealed. Configurations D, E, and F.   E-27366
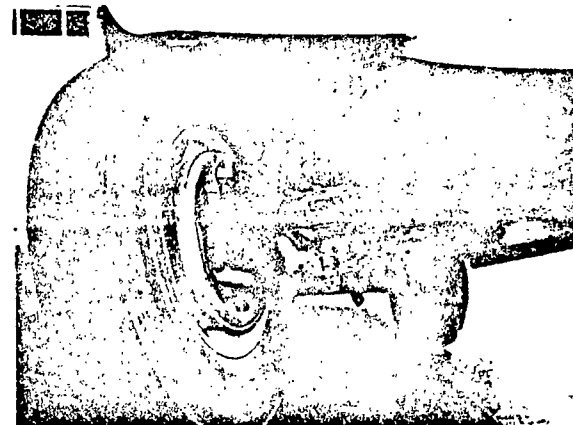
(b) Exposed. Configurations A, B, and C.   E-27721

Figure 9. Right front wheel well, looking rearward.

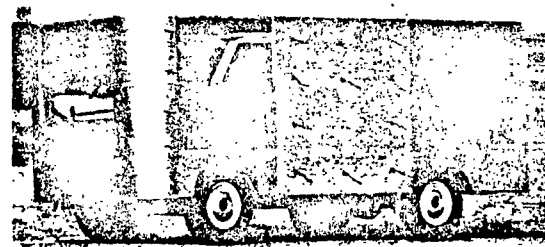(a) Sealed. Configurations D, E, and F.　　E-27224

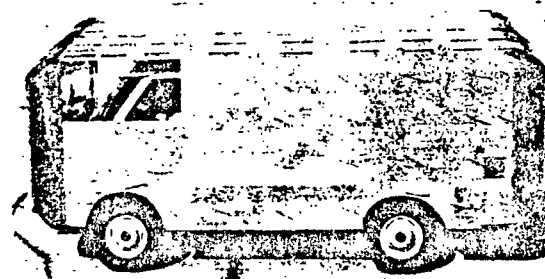(b) Exposed. Configurations A, B, and C.　　E-27225

Figure 10. Rear wheel wells.

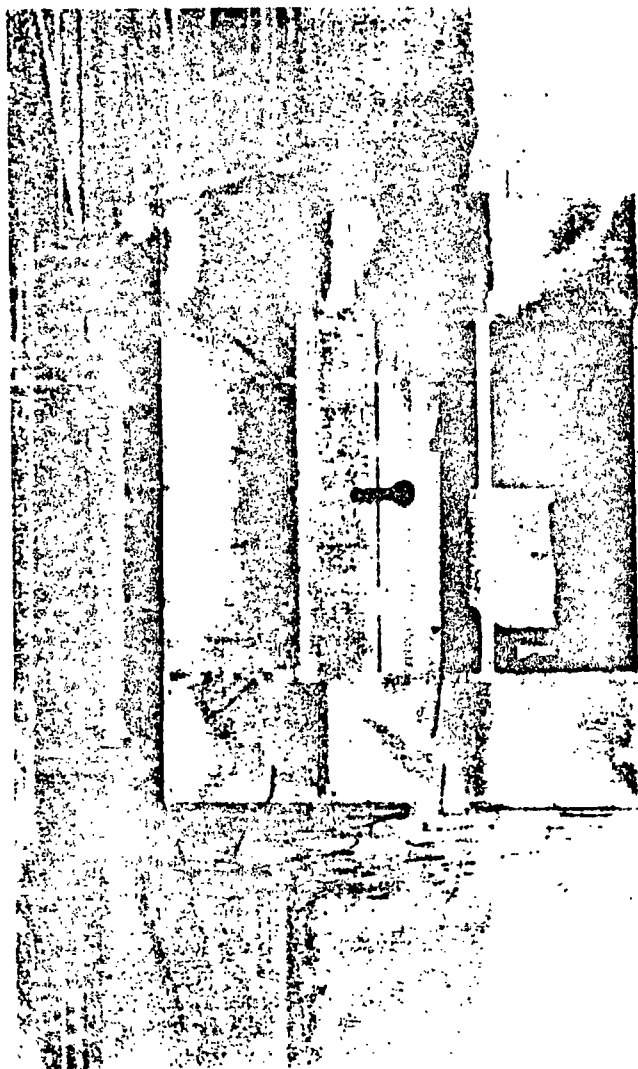(a) Configuration A.　　E-26717

(b) Configuration B.　　E-26903

(c) Configuration C.　　E-27068

Figure 11. Tuft patterns for configurations A, B, and C at a calibrated speed of 55 miles per hour. Cooling vent closed.

Figure 12. Tuft patterns for configuration A at a calibrated speed of 55 miles per hour. Cooling vent closed; front view.
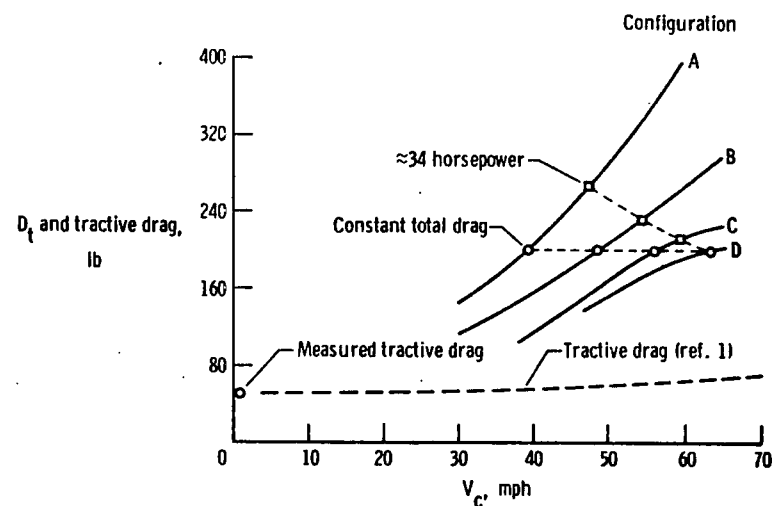
E-26719

Figure 13. Relationship of total drag to velocity. Obtained by the coast-down method with stopwatch-speedometer readings. (The tractive drag does not include the rotational inertia of wheels and tires.)

D_t and tractive drag, lb

≈34 horsepower

Constant total drag

Measured tractive drag

Tractive drag (ref. 1)
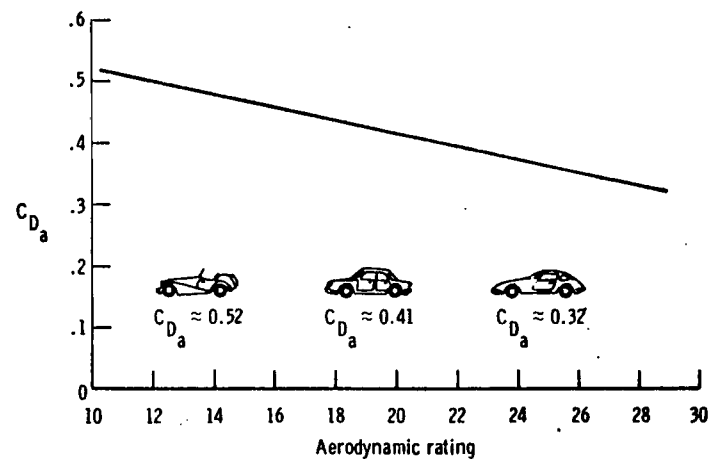
Configuration

V_c, mph

Figure 14. Variation of aerodynamic drag coefficient with automobile type and aerodynamic rating (adapted from ref. 9).

c_{D_a}

$C_{D_a} ≈ 0.52$ $C_{D_a} ≈ 0.41$ $C_{D_a} ≈ 0.32$

Aerodynamic rating